molecular pharmaceutics

Article

pubs.acs.org/molecularpharmaceutics

Enhanced Extravasation, Stability and *in Vivo* Cardiac Gene Silencing via *in Situ* siRNA–Albumin Conjugation

Shannen Lau, Bim Graham, Nga Cao, Ben J. Boyd, Colin W. Pouton, and Paul J. White*

Monash Institute of Pharmaceutical Sciences, Monash University, 381 Royal Parade, Parkville, Victoria, Australia 3052

Supporting Information

ABSTRACT: A potential barrier to progression of siRNA therapeutics to the clinic is the ability of these agents to cross the vascular endothelium to reach target cells. This study aimed to bypass the endothelial barrier by harnessing the extravasation capability of the serum protein albumin to allow siRNA to reach cardiomyocytes. A strategy for conjugating siRNA to albumin *in vivo* was developed that involved activating 3′-amine, 2′-*O*-methyl, phosphorothioate modified siRNA with succinimidyl 4-[*N*-maleimidomethyl]cyclohexane-1-carboxylate (SMCC) to yield maleimide-functionalized siRNA ("activated siRNA"); this thiol-reactive species can then irreversibly link to the single surface-exposed cysteine residue of endogenous albumin following intravenous administration. An IGF-I-receptor (IGF-IR) siRNA sequence which was effective *in vitro* was used to test the ability of the siRNA–albumin conjugate to bypass the endothelial barrier in Balb/C mice and produce silencing. *In situ* conjugation of maleimide-functionalized siRNA to albumin in mouse serum occurred within minutes of addition, and the resulting conjugate was found to be nuclease stable by SDS–PAGE analysis. In Sprague–Dawley rats, activated siRNA showed a significantly enhanced elimination half-life (75.9 ± 18.2 min) compared to unactivated siRNA (5.1 ± 0.2 min). Intravenous injection of this activated siRNA (1 mg/kg daily for four days) significantly reduced left ventricle IGF-IR mRNA to 64.1 ± 4.1% of that in vehicle-treated animals (mean ± SEM), while the control siRNA (unconjugated) had no effect (n = 4, P > 0.05). Imaging of microvessels from mice treated with fluorescein-labeled activated siRNA showed clear evidence of extravasation and cellular uptake in capillary endothelial cells, cardiomyocytes and vascular smooth muscle cells for mice treated with the activated siRNA but not mice treated with the unactivated siRNA. siRNA–albumin constructs are therefore capable of extravasation to the myocardium resulting in silencing in this otherwise silencing-resistant organ.

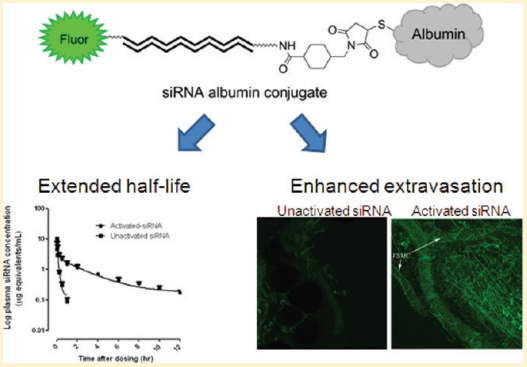

KEYWORDS: *siRNA, albumin, delivery, extravasation*

INTRODUCTION

The extraordinary therapeutic potential of short interfering RNA (siRNA) has generated intensive research activity across a diverse range of biomedical fields, including cardiovascular disease. It is well established that there are a number of biological hurdles to overcome before systemically administered siRNA can reach the cytosol of target cells.[1,2] These include nuclease susceptibility, poor penetration into many tissues (possibly due to limited extravasation), inefficient entry into target cells and finally limited endosomal escape. Thus far, successful silencing in animals has often involved "hydrodynamic injection"[3,4] to bypass barriers to cellular delivery, in which siRNA is administered using extremely large injection volumes. Rational delivery strategies have since been developed, including an elegant combination of siRNA condensation with sperm protamine and specific cell targeting using an HIV envelope antibody.[5] More recently Peer et al. demonstrated the capabilities of nanoparticles containing siRNA and a targeting antibody.[6] While there are a number of other examples of successful siRNA-mediated silencing after systemic administration, these have largely been limited to the liver, lung and kidney, organs in which particulate or naked siRNA accumulates in significant concentrations. A generic delivery method for RNA interference using systemically administered siRNA remains to be found.

We have previously shown cardiovascular cell types such as vascular smooth muscle cells, endothelial cells and cardiomyocytes to be amenable to gene silencing using systemic administration of naked, nuclease-stable antisense oligonucleotides *in vivo*.[7−9] When attempting to harness the power of siRNA *in vivo*, we found that, unlike single-stranded antisense, fluorescently labeled, nuclease stable siRNA did not penetrate into the myocardium or vascular wall after intravenous administration, and thus we identified poor extravasation as a key impediment to *in vivo* silencing in these tissues. The serum protein albumin was identified as a potential "piggyback" solution. Albumin is known to cycle between blood and lymph

Received: May 13, 2011
Revised: November 28, 2011
Accepted: December 5, 2011
Published: December 5, 2011

Scheme 1

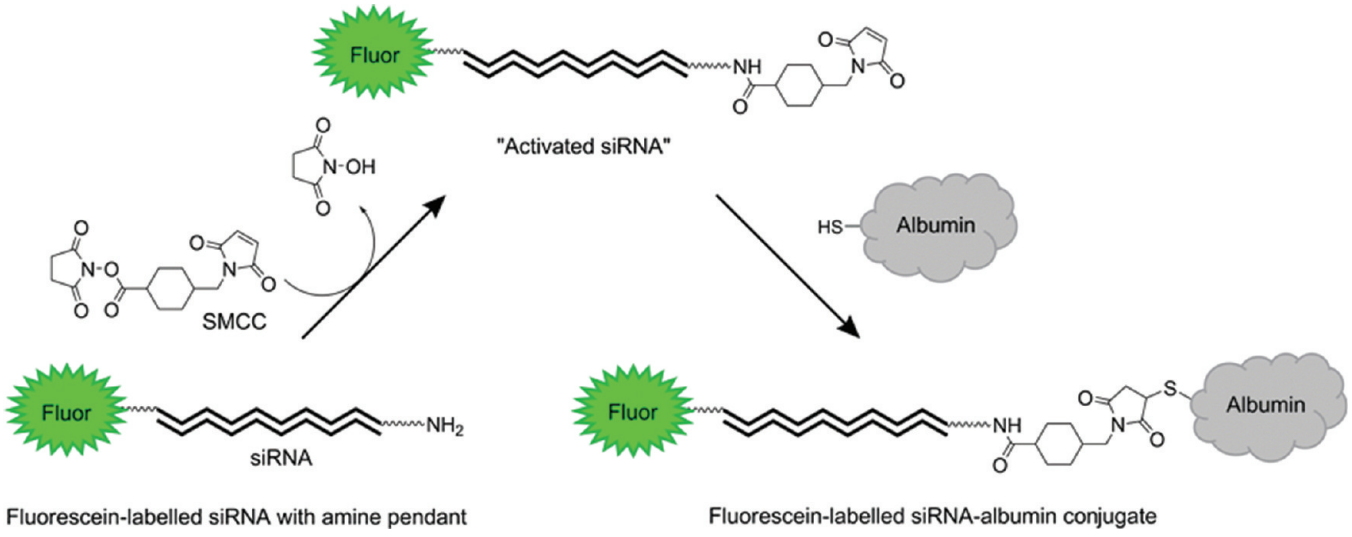

in great quantities; 120−145 g of albumin extravasates per day in humans and is returned to the circulation by lymphatic drainage.[10] Strategies using albumin as a drug carrier have been successful using nanoparticles containing albumin.[11] Cardiac microvessel endothelial cells have been shown to express the albumin-binding protein gp60,[12] thought to mediate caveolin-dependent albumin-mediated transcytosis. Thus we hypothesized that covalent conjugation to albumin would result in extravasation of siRNA. We developed a method to produce well-defined 1:1 siRNA−albumin conjugates *in vivo* that involves reaction between native mouse albumin and administered maleimide-functionalized siRNA, and then sought to determine whether cardiac gene silencing could be produced using such a conjugate.

EXPERIMENTAL SECTION

siRNA. To initially determine the level of gene silencing produced by naked, nuclease stable siRNA in a variety of organs, we used commercially sourced, proprietary-modified siRNA (Ambion "*in vivo stable*" siRNA, Tx, USA). The active sequence used targeted the adenosine A_{2A} receptor ($A_{2A}R$). $A_{2A}R$ siRNA sequences were as follows: 5′-FAM-GACCUUCCGGAAGAUCAUCdTdT-3′ (sense strand) and 3′-dGdTCUGGAAGGCCUUCUAGUAG-′5 (antisense strand), and the mismatch sequence was 5′-FAM-AUAUUUGGAAACAGCUUGGdTdT-3′ (sense strand) and 3′-dCdTUAUAAACCUUUGUCGAACC ′5.

Subsequently, for the imaging and albumin-conjugation experiments, we validated an insulin-like growth factor type I receptor (IGF-IR) siRNA (see Supplementary Figure 1 in the Supporting Information). siRNA were modified to provide nuclease resistance; each sense strand contained four 2′-*O*-methyl (2′-OME) modifications, while the antisense strand contained two 2′-*O*-methyl modified nucleotides, and both strands contained two phosphorothioate (PS) internucleoside linkages. For the tissue distribution studies we used an Alexa 488 nm labeled 2′-OMe(*)/PS(+) duplex (Sigma Aldrich, Sydney, Australia), with the sequence 5′-Alexa488-GCC*C*AUG*UGUGAGAA*GACC+dT+dT-3′ (sense strand), and 3′-dT+dT+CGGGUACACACU*CUUCUG*G-5′ (antisense strand). The same 2′-OMe/PS modified sequence was used for the albumin conjugation studies; in this case an siRNA with an hexylamine group (N6) at the 3′ end (for coupling to SMCC) and a fluorescein label at the 5′ end of the sense strand was purchased from Dharmacon (Lafayette, CO, USA).

Reagents. Succinimidyl-4-(*N*-maleimidomethyl)-cyclohexane-1-carboxylate (SMCC) was purchased from Thermo Scientific (Pierce, Rockford, IL, USA) and dissolved in DMSO at 9.57 mM prior to use. Illustra NAP-5 columns (SephadexTM G-25 DNA grade) were purchased from GE Health Care (U.K.). RNase-free phosphate buffered saline (PBS) pH 7.4 sachets and bovine serum albumin (BSA), mouse serum, Coomassie Brillant Blue and Tris-HCl were purchased from Sigma-Aldrich (NSW, Australia). Primary anti-BSA rabbit IgG antibody, Alexa Fluor 680 donkey anti-rabbit IgG secondary antibody and Ultra pure RNase/DNase free distilled water were obtained from Invitrogen.

An RNA isolation kit "RNeasy Mini Kit" and RNase-free DNase set were obtained from Qiagen (CA, USA). Reagents used for reverse transcription of isolated RNA, included 25 mM $MgCl_2$, 10× PCR Buffer II, Random Hexamer, RNase Inhibitor and Moloney Murine Leukemia Virus (MuLV) reverse transcriptase were obtained from Applied Biosystems (Carlsbad, CA, USA). A dNTP mix was obtained from Roche (New Jersey, USA). Taqman Master mix, eukaryotic rRNA 18s and IGF-IR and $A_{2A}R$ primers for real time analysis were also from Applied Biosystems.

Animals. Experiments were carried out using 20−25 g C57/Bl6 and Balb/C mice, and 200−250 g Sprague−Dawley rats. Animals were housed in plastic cages maintained on a constant 12 h light/12 h dark cycle at 18−22 °C. Food and tap water were provided ad libitum. Experiments were carried out under approval of the Monash University Animal Experimentation Ethics Committee, and in accordance with the Code of Practice of the National Health and Medical Research Council of Australia (seventh edition, 2004).

Synthesis and Characterization of siRNA−BSA Conjugates. The conjugation strategy employed allowed for well-defined 1:1 siRNA−albumin conjugates to be formed both under controlled conditions using pure albumin and also *in situ* using the native albumin derived from the mouse being treated. Commercially sourced 3′-amine and 2′-OMe/PS modified IGF-IR siRNA (1 nmol, 0.2 nM) was first reacted with SMCC (40

dx.doi.org/10.1021/mp2002522 | *Mol. Pharmaceutics* 2012, 9, 71−80

nmol, 9.57 nM) for 1 h at room temperature to yield maleimide-functionalized, thiol-reactive siRNA ("activated siRNA"). Excess SMCC was removed from the thiol-reactive siRNA by gel filtration chromatography using a NAP-5 column (Pharmacia, U.K.). The quantity of filtered thiol-reactive siRNA was determined by fluorescence reading by EnVision multilabel plate reader (USA) with 488 nm excitation/520 nm emission.

The siRNA was then coupled to the single, surface-exposed cysteine-34 residue of albumin via a Michael (conjugate) addition reaction (Scheme 1). The inspiration for this conjugate scheme derived from the work of Kratz,[11,13,14] whose group has employed the same (or similar) strategies to couple several low-molecular weight drugs to albumin (both *in vivo* and *ex vivo*) for targeted delivery to tumors, as well as to couple bioactive peptides/proteins to albumin in order to improve their pharmacokinetic profile

The coupling efficiency of activated siRNA to albumin was first assessed by incubating siRNA with BSA at 2:1 molar ratio for up to 24 h. *Ex vivo* conjugates were then formed in mouse serum at various time points to examine the coupling efficiency and nuclease stability. *In vivo* conjugation using native mouse albumin was performed by intravenous administration of 5 mg/kg activated siRNA in male Balb/C mice (20−25 g). Blood samples were collected 4 h postinjection followed by plasma extraction for conjugation analysis. *Ex vivo* and *in vivo* synthesized conjugates were examined using 10% SDS−PAGE, together with albumin and siRNA standards of known molecular weight (66.5 kDa and 14 kDa, respectively). The gels were loaded at 1 μg of protein or 5 μL of 1% serum per well and run for 90 min at constant 100 V in SDS running buffer. siRNA was visualized under UV light and proteins were visualized following Coomassie Brilliant Blue staining.

Investigation of Activated siRNA Coupling to Albumin by Western Immunoblotting. Synthesized conjugates were assessed for albumin by Western blot to confirm the activated siRNA binds to albumin and not other proteins. Conjugate samples were separated using 10% SDS−PAGE as described above, except that the gels were run along with Odyssey Two-Colour Weight Markers (LI-COR, USA), and 0.5 μg of protein, 5 μL of 2% serum and plasma were loaded instead. Transferrin glycoprotein was used as a negative control. siRNA and siRNA-containing products were visualized under UV light prior to the gel being to transferred to a nitrocellulose (Ba85) membrane (Whatman, USA) using a Bio-Rad Trans-Blot SD Semi Dry Electrophoretic Transfer cell. The membrane was subsequently blocked by incubation in 5% skim milk in Tris-buffered saline Tween-20 (TBST) for 2 h and then incubated with 1:1000 diluted primary anti-BSA rabbit IgG antibody (Invitrogen, Australia) overnight at 4 °C. Following extensive washing with TBST (5 × 5 min), the membrane was incubated with Alexa-680 donkey anti-rabbit IgG secondary antibody (1:15000) for 2 h at room temperature before imaged using an Odyssey Infrared Imaging system (LI-COR, USA). Albumin bands were visualized using the 700 nm channel, while the ladder was visualized using the 800 nm channel.

***In Vivo* Distribution and Cellular Uptake of Nuclease-Stable siRNA.** *Study 1. 2′-OMe/PS Modified, Alexa-488-Labeled siRNA versus Vehicle.* Female Balb/C mice, 20−25 g, were given a single 5 mg/kg dose of 2′-OMe/PS modified, Alexa-488 labeled siRNA via tail vein injection. At 4 h post treatment, tissue was collected and embedded in Tissue-Tek OCT and frozen in dry ice. Tissues imaged included liver, kidney, aorta and left ventricle. Frozen tissue sections (5 μm) for each animal were cut using a Cryostat (Leica CM1850) at 19−21 °C, thaw-mounted onto gelatin (0.5% w/v)/chrome alum (0.05% w/v) coated slides (0.5% w/v). Slides were coverslipped with Vecta-shield (Vecta laboratories, CA, USA) and allowed to incubate for 15 min at room temperature. Cellular uptake and tissue distribution of Alexa-488-labeled siRNA were visualized using fluorescence microscopy (Olympus BX61) and AnalysSIS LS software or confocal microscopy (LSM 510 Meta).

Study 2. Activated 2′-OMe/PS Fluorescein-Labeled siRNA versus Unactivated 2′-OMe/PS-Modified, Fluorescein-Labeled Unactivated siRNA versus Vehicle. Distribution and cellular uptake for the 2′-OMe/PS-modified, fluorescein-labeled siRNA−BSA conjugation study were examined as described above using fluorescein-labeled unactivated (5 mg/kg) and fluorescein-labeled activated siRNA (5 mg/kg) compared to vehicle. We used fluorescein-labeled siRNA for this conjugation study because we were unable to source Alexa488-labeled, 2′-OMe/PS-modified siRNA with the hexylamine modification. Tissue sections were imaged using a Nikon A1R confocal microscope. Mesenteric vasculature whole mounts were used as this tissue provides a simple means of imaging blood vessels of all types, including microvasculature. Whole mounts were produced by removal of excess fat from mesenteric vasculature followed by mounting. Microvessels were identified, and serial z-sections (step size 0.3 μm, total thickness 10−20 μm) were captured under constant laser power and gain settings for all samples. In order to produce a single image for publication, maximum intensity projections from each stack were produced using the Nikon AIS elements software. Cardiac left ventricles were removed and sectioned at 60 μm prior to slide mounting. Confocal imaging was performed as described for mesenteric whole mounts.

***In Vivo* Pharmacokinetics of Activated siRNA in Rats.** The left jugular vein and right carotid artery of male Sprague−Dawley rat were cannulated in order to characterize the *in vivo* pharmacokinetics of activated siRNA. Cannulation procedures were as previously described,[7] except that in this case the animals were anesthetized using isoflurane. The rats were allowed to recover overnight prior to dosing. After the recovery period, rats were housed in metabolic cages to permit separate collection of urine and feces, and the cannulae were attached to a swivel/leash assembly to facilitate drug administration and blood collection. Free access to water was allowed at all times. Freshly prepared activated and unactivated siRNA were injected intravenously at 0.5 mg/kg followed by 0.25 mL of heparinized saline (2 units/mL) to ensure infusion of the entire dose. Blood samples (0.15 mL) were subsequently abstracted from carotid artery at the following nominal time points: prior to dosing (−5 min), at the instant of conclusion of infusion (t = 0) and at 2, 5, 15, 30, 60, 120, 240, 360, 480, 600, 720, 1440 min. Blood samples were placed immediately into tubes containing 10 IU of heparin and centrifuged for 5 min at 3500g. The quantity of siRNA products in plasma (100 μL) was then determined by fluorescence using an EnVision multilabel plate reader (USA) with 488 nm excitation/520 nm emission. Data is expressed as μg equivalents per mL derived from spiked blank plasma standard samples. Plasma concentration−time data was fitted to biexponential equations using nonlinear regression analysis within GraphPad Prism 5 software. Rate constants and corresponding half-lives were determined, as was the area under the curve extrapolated to infinity (AUC→∞).

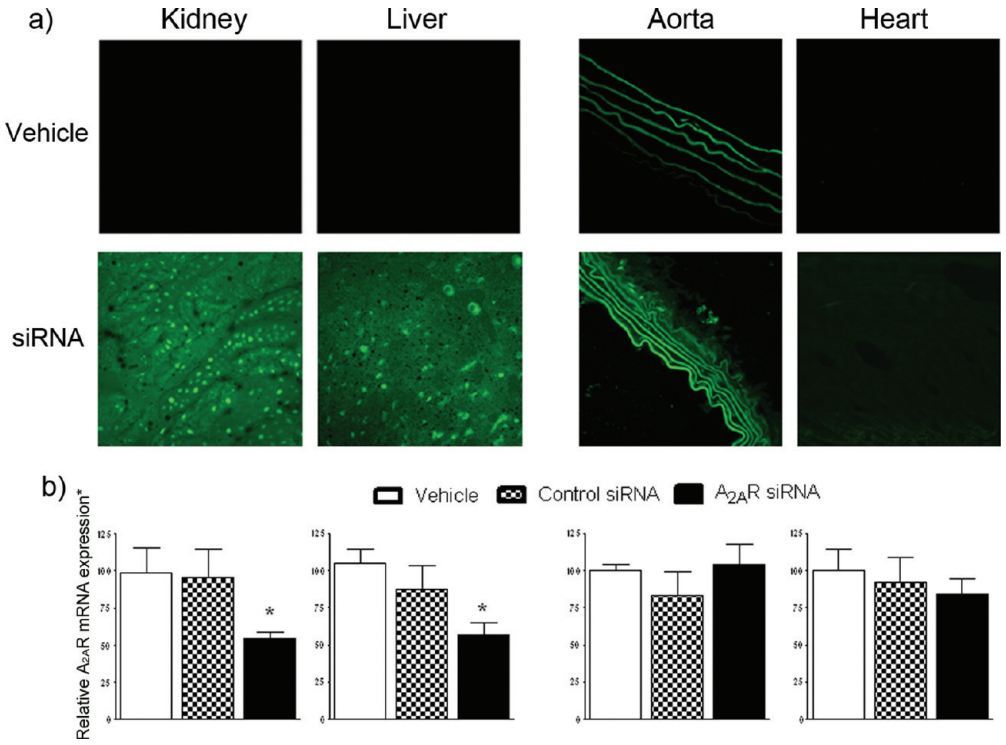

Figure 1. Tissues with discontinuous or fenestrated endothelia show significant extravascular siRNA fluorescence, cellular uptake and target mRNA knockdown. (a) Confocal images of tissue sections from mice treated with vehicle or 5 mg/kg Alexa488-siRNA at 4 h post treatment. Kidney and liver samples show extravascular fluorescence and apparent cellular uptake, while aorta and heart samples showed no significant level of extravascular siRNA. (b) Target ($A_{2A}R$) mRNA expression determined using quantitative real time-PCR relative to vehicle in kidney, liver, aorta and heart for animals treated with vehicle, control siRNA and $A_{2A}R$ siRNA in treated mice ($n = 7-8$). Significant reductions in $A_{2A}R$ mRNA expression level were observed in kidney ($P < 0.05$) and liver samples ($P < 0.05$) of $A_{2A}R$ siRNA treated mice; no significant difference was found in aorta or heart samples. No significant changes in $A_{2A}R$ mRNA expression level were found in mice treated with control siRNA. * Relative $A_{2A}R$ mRNA expression normalized to 18s then to vehicle.

Assessment of *in Vivo* Efficacy of Intravenously Administered Activated siRNA in Mice by Quantitative Real-Time Reverse Transcriptase Polymerase Chain Reaction (QRT-PCR). The silencing efficacy of the activated siRNA was assessed using 25−30 g male Balb/C mice. Tail vein injections of saline or unactivated (0.3, 1, or 3 mg/kg) or activated IGF-IR siRNA (0.3, 1, or 3 mg/kg) were given at 0, 24, 48, and 72 h. Animals were culled and organs were excised at 96 h post treatment for knockdown analysis by quantitative real-time PCR. Tissues collected after 96 h of treatment were snap frozen with liquid nitrogen and stored at −80 °C until further use. Total RNA was extracted from frozen tissues using an RNeasy Mini Kit according to the manufacturer's protocol. During RNA purification, RNA was treated with RNase-free DNase to remove any contaminating genomic DNA. The purity and quantity of extracted RNA were assessed by the absorbance ratio by 260/280 nm using a NanoDrop 1000 spectrophotometer (NanoDrop). 100−500 ng of total RNA per 20 μL of reaction mixture was then reverse transcribed using random hexamers and Moloney Murine Leukemia Virus (MuLV) reverse transcriptase to synthesize template cDNA (cDNA). The relative abundance of target (IGF-IR/$A_{2A}R$) or comparator (adenosine $A_{2A}R$ or AT_1R) mRNA product in tissue samples were determined by real time PCR using thermal cycler Rotor-Gene 3000 (Corbett Research). cDNA was amplified in the presence of specific primers (IGF-IR and A_{2A} receptor) with eukaryotic rRNA 18s as the internal control under manufacturer's protocol. Knockdown was determined by comparison of mRNA level in activated siRNA-treated animals with that in vehicle-treated animals. siRNA knockdown was demonstrated by a reduction in the ratio of the target gene mRNA level to the house keeping gene (18s), and the specificity of knockdown also evaluated using the comparator ($A_{2A}R/AT_1R$) gene expression level.

Statistical Analysis. Plasma pharmacokinetic parameters were compared using an unpaired *t* test using a computer program, GraphPad Prism 5. The effect of siRNA administration on mRNA levels was also calculated using GraphPad Prism 5. Statistical significance for this data was determined by one-way analysis of variance (ANOVA) followed by Dunnett's post test for significant differences between groups for parametric data sets. A *P*-value of less than 0.05 was considered to indicate statistical significance. Data in graphs are presented as mean ± standard error of the mean (SEM), and *n* represents the number of animals per group.

RESULTS

Assessment of siRNA Extravasation and Silencing in Organs with Continuous and Discontinuous Endothelia. The tissue distribution and cellular uptake of an Alexa488-labeled, 2′-*O*-methyl/phosphorothioate modified siRNA duplex were determined after intravenous administration (5 mg/kg, Figure 1a). The Alexa 488 nm fluorophore was chosen as previous pilot studies using fluorescein-labeled siRNA resulted in fluorescence levels barely above the limits of detection in organs such as the heart. Intravenous administration of Alexa-488-labeled siRNA resulted in significant extravascular fluorescence in the kidney and liver, organs with fenestrated/

dx.doi.org/10.1021/mp2002522 | *Mol. Pharmaceutics* 2012, 9, 71−80

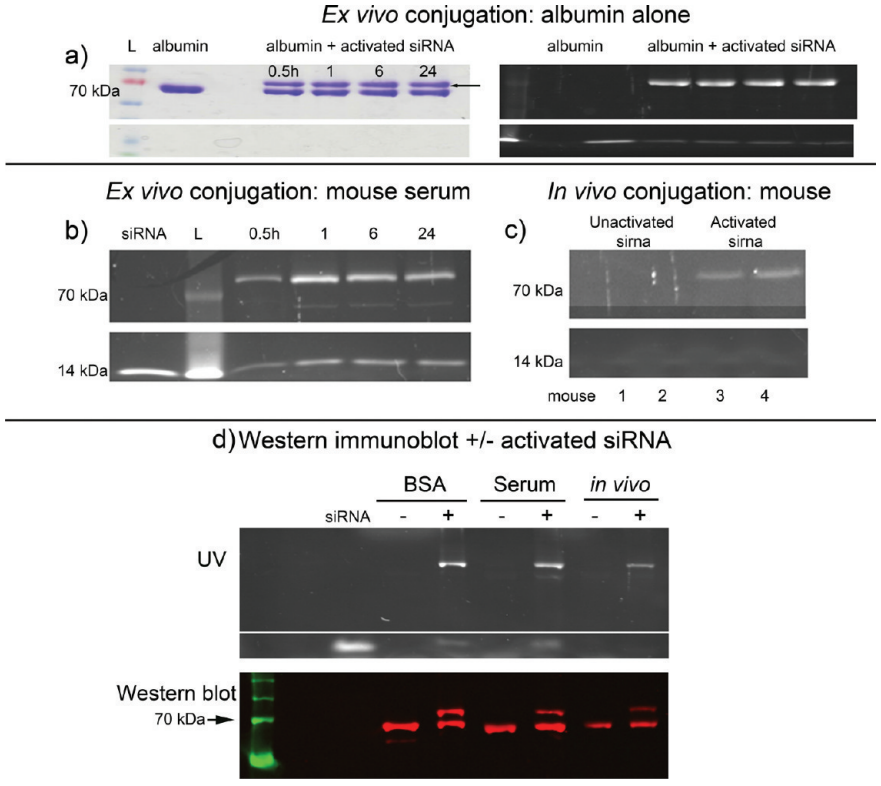

Figure 2. siRNA conjugation with albumin was successful *ex vivo* and *in vivo*. (a) PAGE gels showing conjugation of siRNA with albumin *ex vivo*; arrow indicates conjugate of predicted size. *Ex vivo* conjugation of siRNA with albumin results in two bands after Coomassie staining (left); the higher molecular weight band was also evident under UV exposure, indicating the presence of the siRNA. (b) Incubation of activated siRNA in mouse serum resulted in increasing conjugate production over time. (c) Plasma samples from two mice treated with activated siRNA show evidence of the conjugate, while two mice treated with unactivated siRNA do not. (d) Upper panel shows conjugate bands evident under UV exposure when activated siRNA was added to BSA or serum or injected intravenously. Lower panel shows corresponding western immunoblots using antialbumin antibody, in which the native albumin and the conjugate show albumin imunnoreactivity. L: protein ladder.

sinusoidal endothelia. Confocal imaging showed clear cellular siRNA uptake in each of these tissues (Figure 1a, second panel). In these organs there was little tissue autofluorescence under the capture conditions used (<10% laser power, amplification gain constant), as evidenced by the low background fluorescence in vehicle-treated samples. Within the heart, fluorescence in sections from Alexa488-labeled siRNA-treated animals was similar to autofluorescence seen in sections from vehicle-treated animals, and there was no fluorescence clearly associated with cells (Figure 1a). Alexa488-labeled siRNA was not detectable within aortic medial layers after intravenous injection (Figure 1a; note that collagen/elastin autofluorescence is visible as concentric rings).

To assess the correlation between *in vivo* distribution of siRNA and subsequent gene silencing, we treated mice with 5 mg/kg $A_{2A}R$ siRNA, control siRNA or vehicle at 0 and 48 h and knockdown was examined at 96 h post treatment. The $A_{2A}R$ siRNA sequence used was shown to be effective and selective *in vitro* (see Supplementary Figure 1 in the Supporting Information). Figure 1b shows the target gene ($A_{2A}R$) mRNA levels after 96 h. A significant reduction of $A_{2A}R$ mRNA level was observed in $A_{2A}R$ siRNA treated kidney samples (mRNA expression reduced to 54.3 ± 4.5% of that in vehicle, mean ± SEM, $P < 0.05$, $n = 7–8$, Figure 1b) and liver samples (mRNA expression reduced to 56.6 ± 8.4% of control, $P < 0.05$, $n = 7–8$, Figure 1b). No significant changes in $A_{2A}R$ expression were observed in aorta samples (Figure 1b, $n = 7–8$, $P > 0.05$). mRNA expression levels of the comparator cell surface receptor (AT_1R) were unchanged by either $A_{2A}R$ siRNA or control siRNA (Supplementary Figure 2 in the Supporting Information).

Conjugation of Nuclease-Stable siRNA to Albumin Occurs *ex Vivo* and *in Vivo* Using Maleimide-Functionalized siRNA. The siRNA–albumin conjugation was initially performed using siRNA with purely unmodified nucleotides, however the resulting conjugates were not stable in the presence of serum due to nuclease degradation (Supplementary Figure 3 in the Supporting Information), and thereafter nuclease-stable, 2′-OMe/PS modified siRNA were used. Using SMCC-activated 2′-*O*-Me/PS modified, fluorescein-labeled siRNA (activated siRNA; see Experimental Section for description), the conjugation reaction occurred predictably; separation of reactants from conjugate using PAGE resulted in a Coomassie-stained band running more slowly than the unreacted albumin (Figure 2a left panel). This band was detected under UV light, indicating the presence of the siRNA, and ran at the expected size for a 14 kDa siRNA conjugated with a 66.5 kDa protein (Figure 2a, right panel). The amount of product peaked at 1 h reaction time using purified bovine serum albumin (Figure 2a). When the reaction was performed using mouse serum rather than bovine albumin, a band at ~80 kDa was again detected under UV, and the conjugate production again peaked after 1 h incubation with only very small amounts of unreacted siRNA detected (Figure 2b). Finally, Balb/C mice were injected with 5 mg/kg activated siRNA to determine whether the conjugate could be produced

dx.doi.org/10.1021/mp2002522 | *Mol. Pharmaceutics* 2012, 9, 71–80

in vivo (Figure 2c). Serum from mice taken 4 h after intravenous administration of activated siRNA indicated the same ~80 kDa band detectable under UV exposure, while there was no band evident in mice treated with the unactivated (amine-modified) siRNA (Figure 2c). To confirm that the electrophoretic band did indeed represent siRNA conjugated to albumin, a Western immunoblot was performed. Figure 2d shows the gel scan under UV, in which the conjugate can be seen in samples where activated siRNA has been added to pure BSA or mouse serum, and finally after intravenous injection. Figure 2d (bottom panel) shows the immunoblot, in which the activated siRNA samples show immunoreactive bands for both the native albumin and the putative siRNA–albumin conjugate band. Thus, the data indicate that activated siRNA, when introduced into mouse serum or mouse blood, forms a conjugate with albumin and does not appear to react with other proteins.

The plasma concentration–time profiles for activated and nonactivated siRNA in Sprague–Dawley rats were determined (Figure 3). The resulting pharmacokinetic parameters were

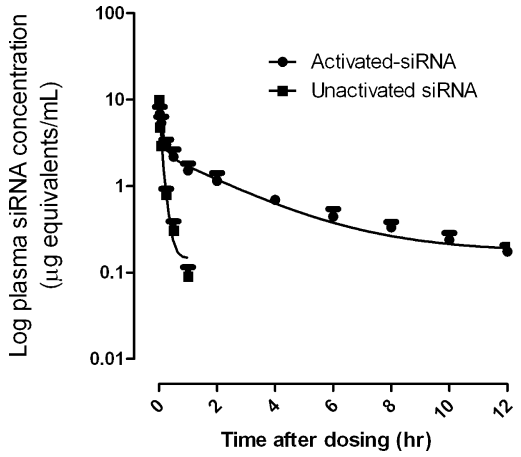

Figure 3. Conjugation to albumin extends plasma half-life in of siRNA in rats. Plasma concentration of activated and unactivated siRNA following intravenous administration at a dose of 0.5 mg/kg to rats (mean ± SD, n = 4–5). Activated siRNA showed significantly increased plasma concentrations between 0 and 2 h post intravenous injection compared to unactivated siRNA treated animals; n = 5. The data are shown as μg equivalents/mL of administered siRNA.

Table 1. Plasma Pharmacokinetic Parameters for Activated and Unactivated Fluorescein-Labeled, 2′-OMe/PS-Modified siRNA after Intravenous Administration*

	$T_{1/2}\alpha$ (min)	$T_{1/2}\beta$ (min)	AUC→∞ (μg/mL·h)
unactivated siRNA	0.7 ± 0.1	5.1 ± 0.2	1.0 ± 0.1
activated siRNA	4.0 ± 0.7*	75.9 ± 18.2*	9.2 ± 0.7*

*Data are mean ± SEM, n = 4–5. * indicates a significant difference from the unactivated siRNA (unpaired t test, n = 4–5, $P < 0.05$).

calculated and are shown in Table 1. Unactivated siRNA showed a typically rapid clearance; plasma levels fell more than 90% within 15 min post administration. Plasma concentrations of activated siRNA were significantly greater than that for unactivated siRNA at all time points (two way ANOVA, $P < 0.05$). Using a two-compartment model of nonlinear regression, the area under the plasma concentration–time curve (AUC→∞) was around 9-fold greater for the activated siRNA than the unactivated (Table 1, unpaired t test, $P < 0.05$, n = 4–5), and the half-life was profoundly increased (Table 1, unpaired t test, $P < 0.05$, n = 4–5).

***In Vivo* Conjugation Results in Extravasation of siRNA and Uptake into Cells beyond the Vascular Endothelium.** The mesenteric circulation was used to assess extravasation of fluorescein-labeled activated siRNA, using tissue whole-mounts containing the full range of arteries, veins and capillaries. All vessel types were imaged, but the major focus was capillaries and capillary venules, as these vessels express the greatest levels of the albumin binding protein required for extravasation.[12] Confocal imaging of mesenteric vessels from vehicle-treated animals showed some tissue autofluorescence at 488 nm excitation as expected from connective tissue within the vessel (Figure 4a). Vessels from animals treated with unactivated siRNA showed similar tissue autofluorescence to vehicle-treated animals (Figure 4b). Vessels from animals treated with activated siRNA showed striking fluorescence from capillary endothelial cells and vascular smooth muscle cells in each animal treated (Figure 4 c,d). Fluorescence was evident in microvessel endothelial cells (see arrows, Figure 4c), indicating uptake of the conjugate by the endothelium, and in vascular smooth muscle cells (Figure 4 d), indicating that extravasation of the conjugate had occurred. Similar observations were also observed in myocardium, where enhanced localization of siRNA was observed in ventricular wall of animals treated with activated siRNA (Figure 4 g,h). Autofluorescence in the low power images (Figure 4e–g) was present, however there was a clear increase in extravascular fluorescence in the outer layers of cardiac muscle under low power in hearts from animals treated with activated siRNA (Figure 4g), and under higher magnification this was seen to be cardiomyocyte-associated (Figure 4h). Administration of the unactivated siRNA resulted in little fluorescence above background, and no clear cell-associated fluorescence within vascular cells (Figure 4f). These data indicate that the siRNA–albumin conjugate produced *in vivo* is able to extravasate and be taken up into cells beyond the vascular endothelium.

Systemic Administration of siRNA–Albumin Conjugate Results in Silencing in Mouse Myocardium. In order to determine whether the observed enhanced circulation time, extravasation and cellular uptake reported above resulted in silencing in a tissue containing vessels with continuous and fenestrated endothelia, we measured target (IGF-IR) levels in the heart, kidney, liver and aorta for animals treated with 1 mg/kg activated siRNA, unactivated siRNA or vehicle only (Figure 5). The siRNA sequence used was thoroughly evaluated, with significant knockdown occurring at 20 nM siRNA in cultured cardiomyocytes and no effect on house-keeping gene (18s) or comparator cell-membrane protein ($A_{2A}R$) expression (Supplementary Figure 1 in the Supporting Information). Mice treated with 1 mg/kg activated siRNA showed significantly reduced levels of cardiac IGF-IR mRNA compared to vehicle-treated or unactivated siRNA control-treated animals (ANOVA, n = 4, $P < 0.05$). For the heart samples, we investigated the dose-responsiveness of the knockdown over a small range of doses, and found that the response to 1 mg/kg was greater than that of 0.3 mg/kg and that the response to 3 mg/kg was not greater than that for 1 mg/kg.

In contrast to the heart, treatment with the unactivated siRNA caused a significant reduction in target mRNA levels (n

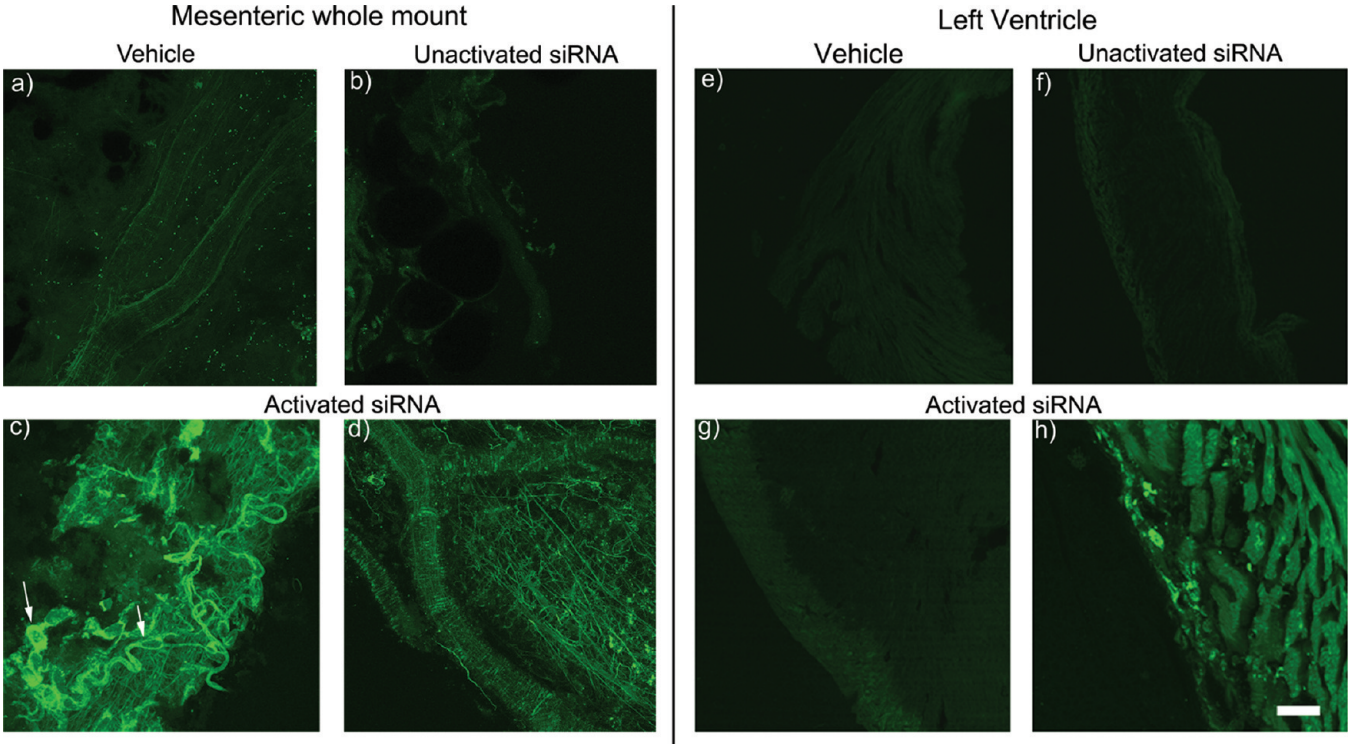

Figure 4. Conjugation to albumin results in extravasation and cellular uptake in mesenteric microvessels and within the left ventricle. (a–d) Images from mesenteric vasculature whole-mount: (a) Autofluorescence from vehicle-treated vessels. (b) The unactivated fluorescein-labeled siRNA (5 mg/kg) was not evident in cells of the vascular wall. (c, d) Activated fluorescein-labeled siRNA (5 mg/kg) administration resulted in uptake into microvessel endothelial cells and vascular smooth muscle cells in mesenteric vasculature whole mounts imaged using confocal microscopy. (e–h) Images from left ventricle samples: (e) Autofluorescence from vehicle-treated vessels. (f) The unactivated fluorescein-labeled siRNA (5 mg/kg) showed vague fluorescence slightly above background but no clear cell association. (g) Activated fluorescein-labeled siRNA (5 mg/kg) resulted in greater extravascular fluorescence in the outer myocardium, which under higher magnification was cell associated (h). Scale bar: (a–d, h) 10 μm; (e–g) 100 μm.

= 4, $P < 0.05$) in mouse kidney samples, while kidney samples from mice treated with the activated siRNA showed a trend toward reduction that was not statistically significant ($n = 4$, $P > 0.05$). Despite a trend toward reduced mRNA levels in liver samples from both activated siRNA-treated animals and unactivated siRNA-treated animals, there were no significant differences between these groups and the vehicle-treatment group. There was no significant effect of either activated or unactivated siRNA from aortas of treated animals ($n = 4$, $P > 0.05$).

DISCUSSION

Extravasation has been previously suggested, without direct evidence, to be a factor that limits siRNA effectiveness after systemic administration.[1,2] Model polymers such as dextran have been used to investigate extravasation, and these show efficient extravasation from blood to lymph for molecules with size below 40 Å radius, through abundant small pores.[15] Thus, siRNA molecules, which would be expected to have a hydrodynamic radius well below 40 Å, should readily cross the vascular endothelium. However, the low levels of siRNA in organs other than liver, kidney and spleen after intravenous administration of naked siRNA has led to the suspicion that siRNA are slow to cross the vasculature in many organs. Also, as argued by Juliano and colleagues, the hydrodynamic radius of charged siRNA species is likely to be greater than that of uncharged dextran polymers.[1] Our data provide evidence that siRNA delivery is severely limited by poor extravasation. Figure 1 of the present study shows that the liver and kidney—organs with discontinuous endothelia—exhibit significant extravascular and cell-associated siRNA fluorescence 4 h after intravenous administration. Furthermore, significant reductions in target gene expression are seen in the liver and kidney using nuclease-stable naked siRNA. In contrast, organs with continuous endothelia—the heart and vascular wall—showed little or no extravascular siRNA and no reduction in target mRNA after systemic treatment with nuclease-stable siRNA. Thus, it appears that delivery strategies to bypass the microvascular endothelium are required for successful siRNA delivery to the heart. Moreover, cellular uptake is sufficient to produce modest (~50%) target knockdown should the siRNA reach the interstitium, at least in some tissue types.

The reticuloendothelial system may have played a role in the high levels of siRNA found in the liver as tissue macrophages are known to take up siRNA.[16] However, specific cellular uptake was also evident within the liver parenchyma. The passive cellular uptake mechanism appeared to allow access of the siRNA to the RNA-induced silencing complex, as we observed a significant reduction in $A_{2A}R$ expression in the liver of mice treated with $A_{2A}R$ siRNA for 48 h. These data may also in part explain why most success *in vivo* using systemic siRNA administration has occurred in the liver, in tumors with altered vascular permeability,[17] or in blood cells.[6,18] Interestingly, hydrodynamic injection,[3,4] conjugation to cholesterol[19] and lipid particle encapsulation of siRNA[20] have been utilized *in vivo*, and current clinical trials of siRNA therapy for liver targets

dx.doi.org/10.1021/mp2002522 | *Mol. Pharmaceutics* 2012, 9, 71–80

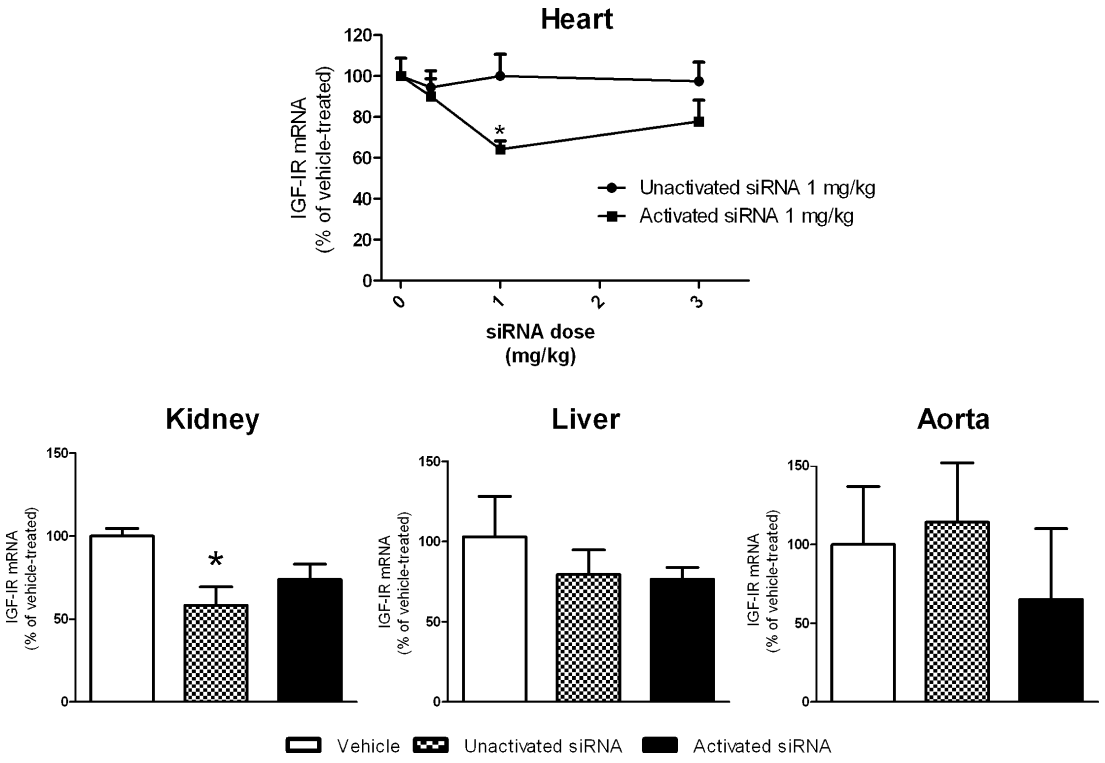

Figure 5. The siRNA–albumin conjugate produced target knockdown in mouse myocardium after intravenous administration. Tail vein injection of activated siRNA daily for 4 days resulted produced a significant reduction in target expression (IGF-IR, normalized to 18s mRNA then to levels from vehicle-treated animals) at 1 mg/kg as assessed by quantitative real-time RT-PCR, while the unactivated/control siRNA had no effect. In kidney samples, the unactivated siRNA reduced target gene expression, while there was no significant effect of the activated siRNA in this tissue. * indicates $P < 0.05$, $n = 4–8$.

involve conjugation to cholesterol or particulate siRNA, suggesting that a higher level of cytoplasmic siRNA is required for optimal silencing than that produced using uncomplexed siRNA. siRNA are clearly able to pass into the renal filtrate, as evidenced by the significant concentration in the urine. From the filtrate, siRNA appears to be internalized by the renal tubular epithelium, as siRNA uptake in these cells was found to be extensive in the present study. The localization was consistent with silencing observed in kidney samples in this study, and with silencing reported in renal tubules by Van de Water and colleagues.[21]

Data from the present study suggest that siRNA conjugation to albumin can occur *in vitro* and *in vivo*. The resultant conjugate remains in the blood for longer periods post administration, and the conjugate does indeed extravasate. The conjugation reaction was found to be efficient. *In vitro*, the reaction resulted in a single band at the expected conjugate size (80 kDa) in PBS and in mouse serum (Figure 2). The presence of some unreacted albumin was not surprising, given that a fraction of albumin is always unavailable; the cysteine-34 residue is blocked in 20–60% of albumin molecules by thiol-containing compounds such as cysteine, homocysteine or glutathione.[22] We recently reported optimization of the reaction conditions, such that between 50 and 100% of siRNA was conjugated.[23]

The conjugation was also successful *in vivo*, as evidenced by a single electrophoretic band at the expected conjugate size in plasma samples taken from animals 4 h after intravenous administration of the activated siRNA (Figure 2c). Western blotting using an anti-albumin antibody was then used to confirm that the conjugate band did indeed represent siRNA conjugated to albumin. This specificity of reaction of maleimide functional groups with albumin in serum is in agreement with the work of Kratz and colleagues, who used HPLC analysis and mass spectrometry to show reaction of a maleimide derivative of doxirubicin with thiolated albumin in human serum.[14]

That siRNA conjugation to albumin reduced plasma clearance was indicated by the observation that siRNA–albumin was still detectable at the expected size via electrophoresis at 4 h; in contrast unconjugated siRNA is not detectable in plasma after 30 min via this method due to rapid renal excretion. We also directly determined the pharmacokinetic behavior of the activated and unactivated siRNA in the rat. The unactivated siRNA showed similar plasma pharmacokinetic properties to that of nuclease-stable naked siRNA previously examined,[24] with siRNA elimination largely complete within minutes. A significant reduction in the rate of plasma clearance of the conjugate-forming activated siRNA was evident, with a prolonged elimination phase compared to the unactivated siRNA (Figure 3 and Table 1). The elimination half-life of the activated siRNA (~75 min) was similar to that of siRNA-cholesterol conjugates reported by Soutschek and colleagues[19] (95 min). Interestingly, Soutschek and colleagues[19] hypothesized that the prolonged plasma kinetics were due to the high level of binding to serum albumin that these workers demonstrated for their conjugates. Thus, activated siRNA demonstrated a significantly enhanced half-life; the "window of opportunity" for extravasation and efficacy was greater. As established by Kratz,[11] the conjugation reaction occurs selectively *in vivo* by virtue of the fact that the majority of circulating proteins do not contain free thiols on their

surface, combined with the fact that albumin is the dominant plasma protein.

We saw siRNA fluorescence within the heart and within cardiomyocytes from animals treated with nuclease-stable, activated siRNA, and significant target knockdown with a relatively low siRNA dose. There are few reports of successful silencing in the myocardium using naked siRNA administration *in vivo*; such studies have employed viral gene delivery,[25] liposomal[26] or amine-containing[27,28] commercial transfection reagents unsuitable for use in siRNA therapeutics. The data from Figures 4 and 5 show that the siRNA−albumin conjugate extravasates effectively, resulting in silencing in the heart, while unconjugated siRNA of the same sequence and modification does not. The lack of significant silencing in the kidney using the activated siRNA may be a result of reduced siRNA reaching the glomerular filtrate, as the size of the conjugate would be expected to be greater than the cutoff for glomerular filtration. It was unclear whether extravasation occurred in the vascular wall for siRNA−albumin conjugate. There was little extravascular fluorescence above background in the aortas or mesenteric arteries from animals treated with activated fluorescein-labeled siRNA. However, the background fluorescence in the 488/520 nm channel was sufficient to obscure any low level fluorescence in these samples due to the connective tissue rings within the artery wall. Also, target mRNA levels in aortas of animals treated with activated siRNA showed a trend toward reduced expression which was not statistically significant. The ability of siRNA−albumin conjugates to extravasate in a wide range of organs is currently under investigation.

In summary, we have identified a method of constructing siRNA−albumin conjugates based on activation of amine-modified siRNA with the heterobifunctional linker SMCC and interaction with the surface-exposed cysteine residue on native albumin. Such siRNA conjugates were found to be stable *in vivo*, to extravasate, and to be taken up by vascular endothelial cells and cardiomyocytes. Finally, extravasation of conjugated siRNA was associated with silencing of an exemplar gene target within the myocardium of treated animals. Thus, the use of siRNA−albumin conjugates may be the first generic strategy to allow the extravasation of siRNA and the silencing of target proteins in tissues with continuous endothelia. Strategies to combine enhanced extravasation with methods to overcome the remaining barriers, including cellular uptake and endosomal escape, are the focus of our future research.

■ ASSOCIATED CONTENT

Supporting Information

Supplementary Figure 1 showing that the siRNA used in this study were able to produce specific target mRNA silencing *in vitro*. Supplementary Figure 2 showing a lack of effect of the $A_{2A}R$ siRNA on the expression of a comparator (cell surface protein) gene after intravenous administration. Supplementary Figure 3 showing that siRNA conjugates made from siRNA that are not 2′-*O*-ME/PS modified are rapidly degraded in serum. This material is available free of charge via the Internet at http://pubs.acs.org.

■ AUTHOR INFORMATION

Corresponding Author

*Monash Institute of Pharmaceutical Sciences, Monash University, 381 Royal Parade, Parkville, Victoria, Australia 3052. E-mail: paul.white@monash.edu. Phone: +613 99039074. Fax: +613 99039638.

■ ACKNOWLEDGMENTS

The authors wish to acknowledge the Heart Foundation of Australia Grant-in-aid G-09M 4519 for research support. The authors wish to acknowledge Ms. Danielle Senyschyn for assistance with the Western immunoblotting experiments.

■ REFERENCES

(1) Juliano, R.; Alam, M. R.; Dixit, V.; Kang, H. Mechanisms and strategies for effective delivery of antisense and siRNA oligonucleotides. *Nucleic Acids Res.* **2008**, *36* (12), 4158−71.

(2) White, P. J. Barriers to successful delivery of short interfering RNA after systemic administration. *Clin. Exp. Pharmacol. Physiol.* **2008**, *35* (11), 1371−6.

(3) Lewis, D. L.; Hagstrom, J. E.; Loomis, A. G.; Wolff, J. A.; Herweijer, H. Efficient delivery of siRNA for inhibition of gene expression in postnatal mice. *Nat. Genet.* **2002**, *32* (1), 107−8.

(4) McCaffrey, A. P.; Meuse, L.; Pham, T. T.; Conklin, D. S.; Hannon, G. J.; Kay, M. A. RNA interference in adult mice. *Nature* **2002**, *418* (6893), 38−9.

(5) Song, E.; Zhu, P.; Lee, S. K.; Chowdhury, D.; Kussman, S.; Dykxhoorn, D. M.; Feng, Y.; Palliser, D.; Weiner, D. B.; Shankar, P.; Marasco, W. A.; Lieberman, J. Antibody mediated in vivo delivery of small interfering RNAs via cell-surface receptors. *Nat. Biotechnol.* **2005**, *23* (6), 709−17.

(6) Peer, D.; Park, E. J.; Morishita, Y.; Carman, C. V.; Shimaoka, M. Systemic leukocyte-directed siRNA delivery revealing cyclin D1 as an anti-inflammatory target. *Science* **2008**, *319* (5863), 627−30.

(7) Cao, N.; Lau, S.; Nguyen, T. T.; White, P. J. Characterization of the acute cardiovascular effects of intravenously administered insulin-like growth factor-I in conscious Sprague-Dawley rats. *Clin. Exp. Pharmacol. Physiol.* **2006**, *33* (12), 1190−5.

(8) Nguyen, T. T.; Cao, N.; Short, J. L.; White, P. J. Intravenous insulin-like growth factor-I receptor antisense treatment reduces angiotensin receptor expression and function in spontaneously hypertensive rats. *J. Pharmacol. Exp. Ther.* **2006**, *318* (3), 1171−7.

(9) Nguyen, T. T.; White, P. J. Intravenous IGF-I receptor antisense reduces IGF-IR expression and diminishes pressor responses to angiotensin II in conscious normotensive rats. *Br. J. Pharmacol.* **2005**, *146* (7), 935−41.

(10) Nicholson, J. P.; Wolmarans, M. R.; Park, G. R. The role of albumin in critical illness. *Br. J. Anaesth.* **2000**, *85* (4), 599−610.

(11) Kratz, F. Albumin as a drug carrier: Design of prodrugs, drug conjugates and nanoparticles. *J. Controlled Release* **2008**, *132* (3), 171−83.

(12) Schnitzer, J. E. gp60 is an albumin-binding glycoprotein expressed by continuous endothelium involved in albumin transcytosis. *Am. J. Physiol.* **1992**, *262* (1 Part 2), H246−54.

(13) Kratz, F.; Warnecke, A.; Scheuermann, K.; Stockmar, C.; Schwab, J.; Lazar, P.; Druckes, P.; Esser, N.; Drevs, J.; Rognan, D.; Bissantz, C.; Hinderling, C.; Folkers, G.; Fichtner, I.; Unger, C. Probing the cysteine-34 position of endogenous serum albumin with thiol-binding doxorubicin derivatives. Improved efficacy of an acid-sensitive doxorubicin derivative with specific albumin-binding properties compared to that of the parent compound. *J. Med. Chem.* **2002**, *45* (25), 5523−33.

(14) Kratz, F.; Muller-Driver, R.; Hofmann, I.; Drevs, J.; Unger, C. A novel macromolecular prodrug concept exploiting endogenous serum albumin as a drug carrier for cancer chemotherapy. *J. Med. Chem.* **2000**, *43* (7), 1253−6.

(15) Rippe, B.; Rosengren, B. I.; Carlsson, O.; Venturoli, D. Transendothelial transport: the vesicle controversy. *J. Vasc. Res.* **2002**, *39* (5), 375−90.

(16) Jackson, L. N.; Larson, S. D.; Silva, S. R.; Rychahou, P. G.; Chen, L. A.; Qiu, S.; Rajaraman, S.; Evers, B. M. PI3K/Akt activation is

critical for early hepatic regeneration after partial hepatectomy. *Am. J. Physiol.* **2008**, *294* (6), G1401−10.
(17) Greish, K.; Fang, J.; Inutsuka, T.; Nagamitsu, A.; Maeda, H. Macromolecular therapeutics: advantages and prospects with special emphasis on solid tumour targeting. *Clin. Pharmacokinet.* **2003**, *42* (13), 1089−105.
(18) Peer, D.; Zhu, P.; Carman, C. V.; Lieberman, J.; Shimaoka, M. Selective gene silencing in activated leukocytes by targeting siRNAs to the integrin lymphocyte function-associated antigen-1. *Proc. Natl. Acad. Sci. U.S.A.* **2007**, *104* (10), 4095−100.
(19) Soutschek, J.; Akinc, A.; Bramlage, B.; Charisse, K.; Constien, R.; Donoghue, M.; Elbashir, S.; Geick, A.; Hadwiger, P.; Harborth, J.; John, M.; Kesavan, V.; Lavine, G.; Pandey, R. K.; Racie, T.; Rajeev, K. G.; Rohl, I.; Toudjarska, I.; Wang, G.; Wuschko, S.; Bumcrot, D.; Koteliansky, V.; Limmer, S.; Manoharan, M.; Vornlocher, H. P. Therapeutic silencing of an endogenous gene by systemic administration of modified siRNAs. *Nature* **2004**, *432* (7014), 173−8.
(20) Zimmermann, T. S.; Lee, A. C.; Akinc, A.; Bramlage, B.; Bumcrot, D.; Fedoruk, M. N.; Harborth, J.; Heyes, J. A.; Jeffs, L. B.; John, M.; Judge, A. D.; Lam, K.; McClintock, K.; Nechev, L. V.; Palmer, L. R.; Racie, T.; Rohl, I.; Seiffert, S.; Shanmugam, S.; Sood, V.; Soutschek, J.; Toudjarska, I.; Wheat, A. J.; Yaworski, E.; Zedalis, W.; Koteliansky, V.; Manoharan, M.; Vornlocher, H. P.; MacLachlan, I. RNAi-mediated gene silencing in non-human primates. *Nature* **2006**, *441* (7089), 111−4.
(21) van de Water, F. M.; Boerman, O. C.; Wouterse, A. C.; Peters, J. G.; Russel, F. G.; Masereeuw, R. Intravenously administered short interfering RNA accumulates in the kidney and selectively suppresses gene function in renal proximal tubules. *Drug Metab. Dispos.* **2006**, *34* (8), 1393−7.
(22) Janatova, J.; Fuller, J. K.; Hunter, M. J. The heterogeneity of bovine albumin with respect to sulfhydryl and dimer content. *J. Biol. Chem.* **1968**, *243* (13), 3612−22.
(23) Lau, S.; Graham, B; Boyd, B; Pouton, C. W.; White, P. J. Commercially supplied amine-modified siRNAs may require ultrafiltration prior to conjugation with amine-reactive compounds. *J. Nucleic Acids* **2011**, *2011*, No. 154609, DOI: 10.4061/2011/154609.
(24) Viel, T.; Boisgard, R.; Kuhnast, B.; Jego, B.; Siquier-Pernet, K.; Hinnen, F.; Dolle, F.; Tavitian, B. Molecular imaging study on in vivo distribution and pharmacokinetics of modified small interfering RNAs (siRNAs). *Oligonucleotides* **2008**, *18* (3), 201−12.
(25) Dai, W.; He, W.; Shang, G.; Jiang, J.; Wang, Y.; Kong, W. Gene silencing of myofibrillogenesis regulator-1 by adenovirus-delivered small interfering RNA suppresses cardiac hypertrophy induced by angiotensin II in mice. *Am. J. Physiol.* **2010**, *299* (5), H1468−75.
(26) Arnold, A. S.; Tang, Y. L.; Qian, K.; Shen, L.; Valencia, V.; Phillips, M. I.; Zhang, Y. C. Specific beta1-adrenergic receptor silencing with small interfering RNA lowers high blood pressure and improves cardiac function in myocardial ischemia. *J. Hypertens.* **2007**, *25* (1), 197−205.
(27) Natarajan, R.; Salloum, F. N.; Fisher, B. J.; Kukreja, R. C.; Fowler, A. A. 3rd. Hypoxia inducible factor-1 activation by prolyl 4-hydroxylase-2 gene silencing attenuates myocardial ischemia reperfusion injury. *Circ. Res.* **2006**, *98* (1), 133−40.
(28) Natarajan, R.; Salloum, F. N.; Fisher, B. J.; Ownby, E. D.; Kukreja, R. C.; Fowler, A. A. 3rd. Activation of hypoxia-inducible factor-1 via prolyl-4 hydoxylase-2 gene silencing attenuates acute inflammatory responses in postischemic myocardium. *Am. J. Physiol.* **2007**, *293* (3), H1571−80.